FULL PAPER

Dalton
www.rsc.org/dalton

Photochemical and thermal synthesis and characterization of polypyridine ruthenium(II) complexes containing different monodentate ligands †

Sylvestre Bonnet,[a] Jean-Paul Collin,*[a] Nathalie Gruber,[b] Jean-Pierre Sauvage[a] and Emma R. Schofield ‡[a]

[a] *Laboratoire de Chimie Organo-Minérale, UMR 7513 du CNRS, Université Louis Pasteur, Faculté de Chimie, 4, rue Blaise Pascal, 67070 Strasbourg Cedex, France*

[b] *Service Commun des rayons X, Université Louis Pasteur, Faculté de Chimie, 4, rue Blaise Pascal, 67070 Strasbourg Cedex, France. E-mail: jpcollin@chimie.u-strasbg.fr*

Received 26th August 2003, Accepted 23rd October 2003
First published as an Advance Article on the web 10th November 2003

The photochemical and thermal synthesis of a series of $[Ru(tpy)(phen)L]^{2+}$ complexes where terpy = 2,2′:6′,2″–terpyridine (terpy) or 4-(3,5-di-*tert*-butyl)phenyl-2,2′;6′,2″-terpyridine (terpy*), phen = 1,10-phenanthroline and L monodentate ligands such as Cl^-, NC^-, CH_3CN, pyridine, isoquinoline (iq), 4-dimethylaminopyridine (dmap), 4-(4′-methylpyridinium)pyridine (mqt), phenothiazine (ptz), 3,5-lutidine(lut) and H_2O are described. The complexes have been characterized by ^1H (COSY and ROESY) NMR spectroscopy, mass spectrometry (FAB and ES-MS), cyclic voltammetry, UV-vis absorption and emission spectroscopy and single-crystal X-ray diffraction. Photochemical experiments have shown that the ligands L can be photochemically expelled and replaced by CH_3CN molecules used as solvent. This type of ligand interchange occurs efficiently and very selectively. The reaction has the potential to be applied to a wide range of entering ligands (thioethers, ethers, pyridines, sulfoxides, nitriles, amides) and indicates the high stability of the Ru(terpy)(phen) core under the irradiation conditions.

Introduction

Current interest in the chemistry and particularly in the photochemistry of ruthenium(II) complexes arises from their potential use in solar energy conversion processes,[1] or as components of luminescent sensors,[2] light emitting diodes[3] and more generally photoswitchable molecular devices.[4] In this latter field, reversible light-driven reactions such as photoisomerisation[5] or photosubstitution[6] occurs and could permit the control of large amplitude motion in specially designed systems.[7] In our efforts to develop molecular machines which operate under light irradiation, we recently described different ruthenium systems based on the expulsion of bipyridine or pyridine ligands.[8] As already demonstrated in several ruthenium complexes, the excitation of the MLCT band allows the thermal population of low-lying d–d states from the MLCT excited state and subsequent expulsion of the weaker ligand.[9] In the $[Ru(terpy)(6,6'\text{-dmbp})L]^{2+}$ type complex (terpy = 2,2′:6′,2″-terpyridine, 6,6′-dmbp = 6,6′-dimethyl-2,2′-bipyridine) where L is acetonitrile or pyridine,[8b] a reversible interchange of ligand occurs efficiently and quantitatively. In this paper we will extend the previous study to a series of L ligands including isoquinoline (iq), 4-dimethylaminopyridine (dmap), 4-(4′-methylpyridinium)pyridine (mqt), phenothiazine (ptz), 3,5-lutidine (lut) and H_2O in complexes containing 1,10-phenanthroline and two types of terpyridine: terpy and 4-(3,5-di-*tert*-butyl)-phenyl-2,2′;6′,2″-terpyridine (terpy*).

Results and discussion

Synthesis

Photochemical methods for preparing polypyridine ruthenium complexes are relatively scarce in the literature.[10] This situation is probably the result of the conjunction of unfavourable parameters such as low quantum yields and poor selectivity. A few representative examples[11] involve the $Ru(bidentate)_2$ core, one of the most frequently used chemical subunits in ruthenium(II) chemistry. In this work, photochemical and thermal reactions have both been employed to prepare ruthenium complexes in good yields. The classical thermal route described in the literature[12] allows the preparation of the intermediate compounds $Ru(terpyridine)Cl_3$, $[Ru(terpyridine)(phen)Cl]^+$ and $[Ru(terpyridine)(phen)(CH_3CN)]^{2+}$ as well as the complex **10** (terpyridine = terpy or terpy*). Chart 1 gives the chemical formulae of the compounds synthesized.

By reaction with $AgBF_4$, the precursor of the type $[Ru(terpy)(phen)Cl]^+$ leads to compounds **2** and **9**, conducting the reaction in acetonitrile–H_2O or acetone–H_2O mixture, respectively. Surprisingly, these reaction conditions afforded also, in the case of **2**, a by-product which was identified as $[Ru(terpy)(phen)(CN)]^+$ by determining its X-ray structure. The conditions of formation of this compound remain unclear at the moment. In order to avoid this side reaction some photochemical attempts were made starting from $[Ru(terpy)(phen)Cl]^+$. Irradiation of **1** in CH_3CN–H_2O mixture with white light from a slide projector led to **2** without an isolable amount of **3**. This method turned out to be very efficient and compounds **4**–**8** have been prepared using 10 equivalents excess of the ligand L in deoxygenated acetone. The only exception was the synthesis of **4** which was carried out in neat pyridine.

Crystal structures

The structures of each of the ten cationic complexes have been determined by X-ray crystallography at 173 K. The ORTEP diagrams of compounds **1**–**10** are shown in Fig. 1.

Selected bond lengths and bond angles are given in Tables 1–4.

A number of structures have been published with the general formula $[Ru(terpy)(N–N)L]^{n+}$ where N–N is bipyridine,[9a,13] biquinoline,[14] or bipyrazine[15] and L is a monodentate ligand. Only one structure involves a phenanthroline derivative[16] as bidentate ligand and this is the first time that a systematic series

† Electronic supplementary information (ESI) available: View of the dimeric units of **8** and proton indexation used in the ^1H NMR data. See http://www.rsc.org/suppdata/dt/b3/b310198c/

‡ Present address: Department of Chemistry, Trinity College, College Green, Dublin 2, Ireland.

DOI: 10.1039/b310198c

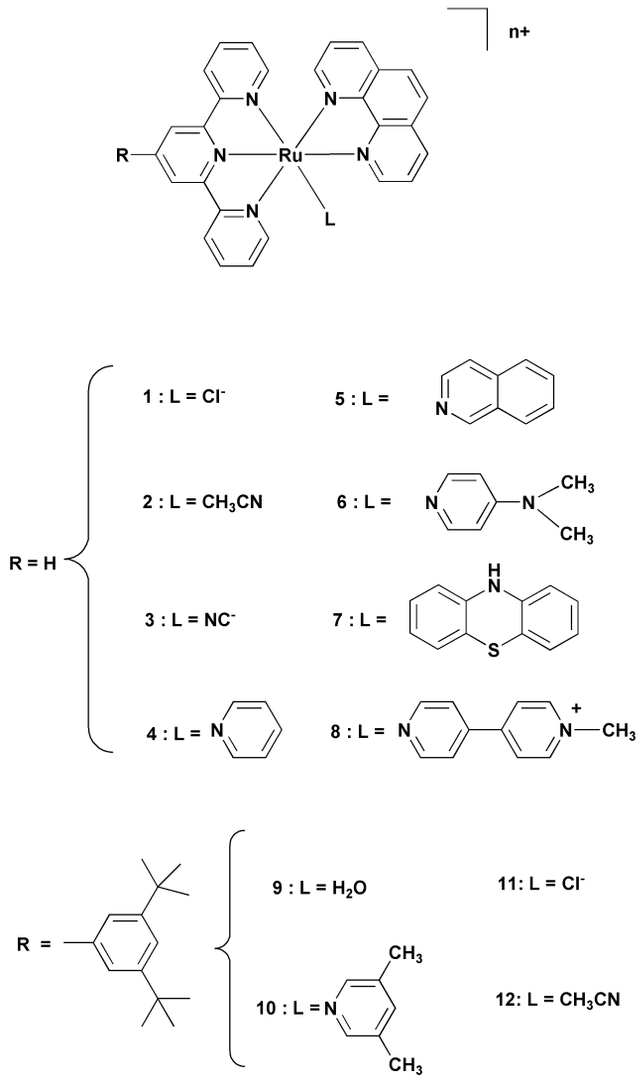

Chart 1

Table 1 Bond lengths (Å) from the ruthenium ion to the coordinating atoms for the complexes **1** to **5**

	1	**2**	**3**	**4**	**5**
Ru–N1	2.105(2)	2.093(4)	2.104(2)	2.112(4)	2.107(4)
Ru–N2	2.051(3)	2.054(4)	2.121(2)	2.074(4)	2.060(4)
Ru–N3	2.074(3)	2.081(4)	2.076(2)	2.088(4)	2.057(4)
Ru–N4	1.961(2)	1.973(4)	1.973(2)	1.981(4)	1.953(4)
Ru–N5	2.084(3)	2.075(4)	2.090(2)	2.078(4)	2.082(4)
Ru–L[a]	2.4180(8)	2.041(5)	2.004(3)	2.113(4)	2.091(4)

[a] L = Cl for **1**; L = C28 for **3** and L = N6 for **2**, **4** and **5**.

Table 2 Bond lengths (Å) from the ruthenium ion to the coordinating atoms for the complexes **6**–**10**

	6	**7**	**8**	**9**	**10**
Ru–N1	2.111(2)	2.104(8)	2.101(9)	2.072(6)	2.106(4)
Ru–N2	2.062(2)	2.069(8)	2.049(8)	2.024(6)	2.056(4)
Ru–N3	2.079(2)	2.068(9)	2.072(8)	2.066(7)	2.070(4)
Ru–N4	1.967(2)	1.956(8)	1.951(9)	1.966(6)	1.963(4)
Ru–N5	2.079(3)	2.056(9)	2.072(9)	2.077(6)	2.068(4)
Ru–L[a]	2.107(2)	2.375(3)	2.100(8)	2.142(5)	2.118(4)

[a] L = S for **7**; L = O1 for **9** and L = N6 for **6**,**8** and **10**.

of structures has been investigated. In all the structures of the present series, the Ru(II) ions are in pseudo-octahedral environments with noticeable asymmetric bond distances to the different coordinated atoms. Characteristic of the Ru(II)–terpyridine complexes, the Ru(II)–nitrogen bond to the central pyridine is shorter than those to the outer two pyridines by 0.1–0.12 Å, as a result of the steric constraint imposed by the tridentate ligand. For a similar reason, the bite angle between the metal and the two outer pyridine rings of the terpy is 158.6–159.3°, *i.e.* significantly smaller than the 180° required for ideal octahedral geometry. Only minor variations in the Ru–N(terpy) bond lengths are observed throughout the series, none of which suggest any significant perturbation by ligand L.

A more significant variation is observed in the Ru–N(phen) bond lengths. In $[Ru(phen)_3]^{2+}$ the average Ru–N(phen) bond length is 2.067 Å.[17] However, looking at this structure in more detail it is apparent that one of the three phen ligands has one short and one long bond to the Ru(II), 2.058 and 2.082 Å, respectively. This is as a result of steric congestion around the metal centre. In the series of structures presented here the two Ru(II)–N(phen) bond lengths are also noticeably different: between the elongated Ru–N bond lengths (2.093–2.112 Å) and the standard axial bond lengths (2.049–2.074 Å) a difference of 0.038–0.052 Å is observed in all complexes except **3**. The observation of one shorter and one longer Ru(II)–N(phen) bond in complexes such as these was originally made for $[Ru(terpy)(bpy)(py)]^{2+}$, in which the difference between the Ru–N bond lengths in the bpy ligand is about 0.04 Å. In this complex, as well as in the novel series discussed here, the longer bond is the one *trans* to the central pyridine of the terpy ligand.[9a] This is

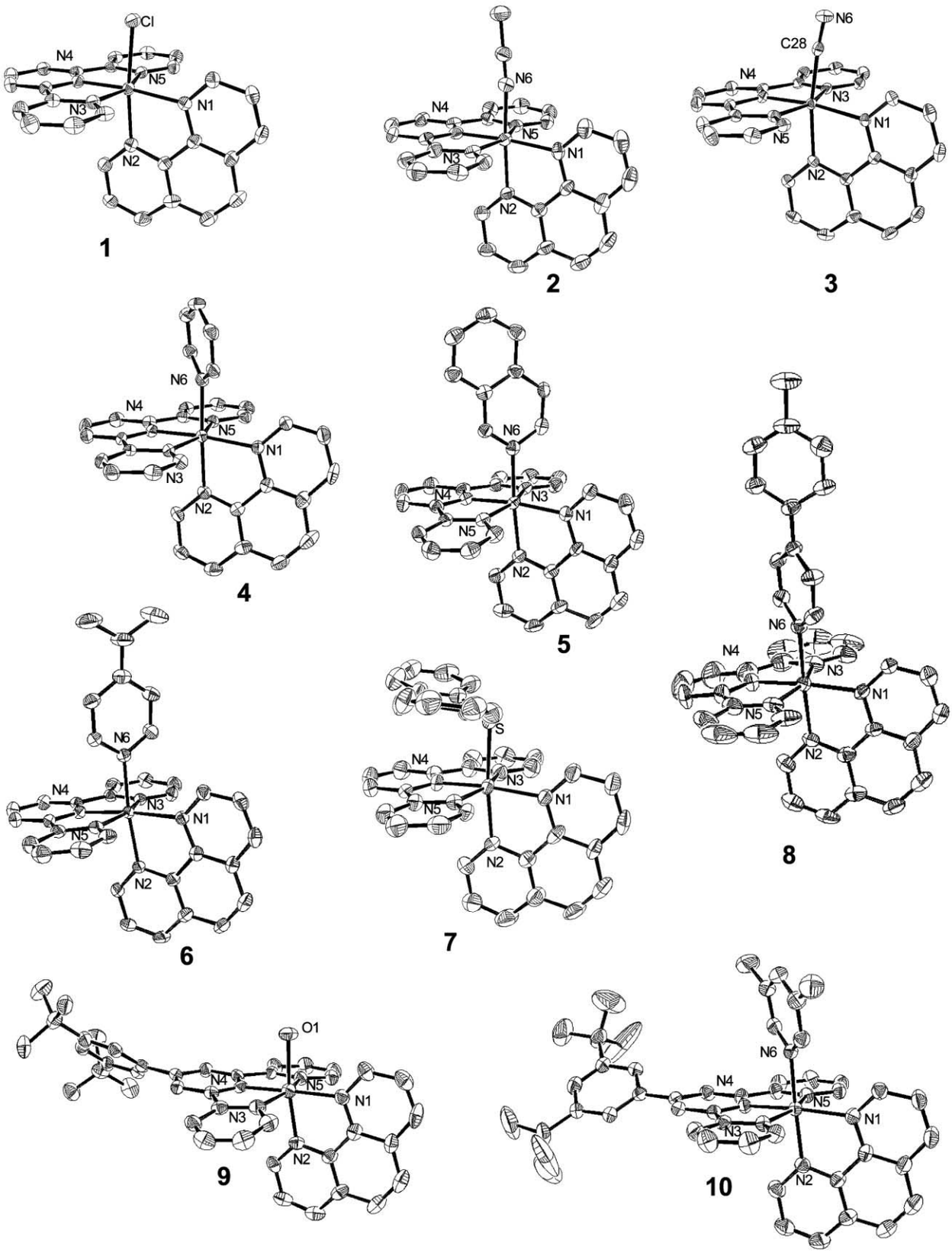

Fig. 1 View of the crystal structures of the ruthenium complexes **1**–**10**. Solvent molecules, H atoms and anions are omitted for clarity. Ellipsoids are scaled to enclose 50% of the electronic density.

also true for the literature structures listed above. In the case of **3**, the equatorial Ru(II)–N(phen) bond is 2.104(2) Å which is again elongated in comparison to $Ru(phen)_3^{2+}$. However, the axial Ru(II)–N(phen) bond is even longer (2.121(2) Å), an observation which cannot be explained by steric crowding, particularly since the same phenomenon is not present in **2** which has the same steric requirements. In **3**, a significant degree of back-bonding to the metal would explain the short Ru(II)–CN bond, the long Ru(II)–N(phen) bond *trans* to the CN and the lack of the same effect in **2**. The Ru(II)–L bond lengths can be compared to those from literature structures containing a different bidentate ligand than phen. In **1**, the Ru–Cl bond length of 2.418(8) Å is similar to that found in analogous complexes such as $[Ru(terpy)(bpz)Cl]^+$ (2.4050(5)

Table 3 Bond angles (°) between the ruthenium ion and the coordinating atoms for the complexes **1**–**5**

	1[a]	**2**	**3**[b]	**4**	**5**
N1–Ru–N2	79.38(9)	79.6(2)	78.66(9)	79.4(1)	79.4(2)
N1–Ru–N3	99.9(1)	101.1(2)	100.31(9)	104.5(1)	98.0(2)
N1–Ru–N4	173.90(9)	174.8(2)	171.73(9)	172.2(1)	173.5(2)
N1–Ru–N5	101.17(9)	99.8(2)	100.97(9)	96.7(1)	102.1(2)
N1–Ru–N6	93.51(7)	95.8(2)	91.9(1)	95.0(1)	95.8(2)
N2–Ru–N3	90.8(1)	88.6(2)	90.67(8)	85.8(1)	88.3(2)
N2–Ru–N4	94.5(1)	95.2(2)	93.08(9)	94.3(1)	94.4(2)
N2–Ru–N5	92.3(1)	93.3(2)	91.87(8)	95.6(1)	89.9(2)
N2–Ru–N6	172.82(7)	175.3(2)	170.6(1)	170.9(1)	175.0(2)
N3–Ru–N4	79.5(1)	79.2(2)	79.35(9)	79.4(2)	79.7(2)
N3–Ru–N5	158.9(1)	159.0(2)	158.7(1)	158.6(1)	159.1(2)
N3–Ru–N6	89.41(7)	91.1(2)	91.7(1)	88.7(1)	93.9(2)
N4–Ru–N5	79.5(1)	79.7(2)	79.35(9)	79.2(1)	79.7(2)
N4–Ru–N6	92.56(7)	89.3(2)	96.3(1)	91.8(1)	90.4(2)
N5–Ru–N6	90.01(7)	88.7(2)	89.3(1)	92.2(1)	89.7(2)

[a] N6 = Cl. [b] N6 = C28.

Table 4 Bond angles (°) between the ruthenium ion and the coordinating atoms for the complexes **6**–**10**

	6	**7**[a]	**8**	**9**[b]	**10**
N1–Ru–N2	79.35(9)	79.5(4)	79.5(4)	80.4(2)	79.4(2)
N1–Ru–N3	102.60(9)	96.5(3)	96.3(4)	102.0(3)	104.3(2)
N1–Ru–N4	174.7(1)	172.1(4)	172.0(3)	177.2(3)	173.7(2)
N1–Ru–N5	98.42(9)	103.9(3)	104.0(4)	98.3(3)	96.4(2)
N1–Ru–N6	94.95(9)	93.4(3)	95.9(3)	90.9(2)	96.2(2)
N2–Ru–N3	90.78(9)	91.6(4)	94.0(3)	88.5(2)	88.8(2)
N2–Ru–N4	95.78(9)	93.3(4)	93.5(4)	97.3(2)	95.7(2)
N2–Ru–N5	90.14(9)	88.3(3)	85.9(3)	89.5(2)	92.1(2)
N2–Ru–N6	173.73(9)	172.8(3)	172.9(3)	171.3(2)	173.4(2)
N3–Ru–N4	79.51(9)	80.1(4)	80.2(4)	79.5(2)	79.3(2)
N3–Ru–N5	158.8(1)	159.2(3)	159.3(4)	159.0(2)	159.1(2)
N3–Ru–N6	87.88(9)	90.6(3)	91.8(3)	92.8(2)	87.6(2)
N4–Ru–N5	79.3(1)	79.2(4)	79.2(4)	80.0(2)	79.8(2)
N4–Ru–N6	90.00(9)	93.8(3)	91.5(3)	91.4(2)	89.1(2)
N5–Ru–N6	93.33(9)	92.2(2)	90.1(3)	92.4(2)	93.3(2)

[a] N6 = S. [b] N6 = O1.

Å),[15] [Ru(tterpy)(mapH)Cl]$^+$ (2.3917(8) Å)[16] and [Ru(terpy)(biq)Cl]$^+$ (2.378(2) Å)[14] (tterpy = 4′-tolyl-2,2′:6′,2″–terpyridine and mapH = 2-anisyl-1,10-phenanthroline). The Ru–$NCCH_3$ bond (2.041(5) Å) is slightly longer than that in [Ru(terpy)(bpy)(CH_3CN)]$^{2+}$ (2.030(10) Å),[13a] while the remaining pyridine-based structures have Ru–L bond lengths in the range of 2.091–2.113 Å which corresponds well to that of [Ru(terpy)(bpy)(pz)]$^{2+}$ (2.091(9) Å) and [Ru(terpy)(bpy)(py)]$^{2+}$ (2.114(6) Å), (pz = pyrazine). In **7**, the side-on coordination type of the PTZ ligand is comparable to that observed in *cis*- or *trans*-[Ru(bpy)$_2$(ptz)$_2$][PF_6]$_2$[18] and [Ru(NH_3)$_4$(mqt)(ptz)][PF_6]$_3$.[19] The Ru–S bond length of 2.375(3) Å and the average of the N–Ru–S bond angles in **7** are also similar to these complexes. In **9**, the Ru–O(H_2O) distance, 2.142(5) Å is found to be almost identical to that in the complex [Ru(terpy)(2-phenylazopyridine)(H_2O)]$^{2+}$ (2.140(5) Å)[20] but slightly longer than in other related complexes.[21]

Although there is no close analogue of [Ru(terpy)(bpy)(mqt)]$^{2+}$ already published, the value of 2.097(3) Å for the Ru–N(mqt) bond length of *trans*-[Ru(NH_3)$_4$(ptz)(mqt)]$^{3+}$[19] is close enough to that of **8** (2.100(8) Å) to suggest that the complex is not distorded. Interestingly, complex **8** forms dimeric units which are arranged in interlocked sheets separated by counterions and solvent molecules (see ESI †). The major difference between the two units in the dimer is the degree to which the mqt is twisted out of the plane of the phen, 47 and 62°, and the extent of twisting between the two pyridyl rings of the mqt unit which is 42 and 30°. Given the large degree of twisting within the ligand and the intra-ring bond length of 1.47 Å, which is significantly longer than the inter-ring bonds (1.35 Å), it seems reasonable to conclude that there is only limited electronic delocalisation within this ligand, although in solution it will undergo free rotation. As already observed before in similar compounds,[13a] another consequence of the packing effect is a distortion in the planarity of the terpyridine ligand occuring in complexes **5** and **9**. This is probably due to the overlap between the terpyridine rings of neighbouring molecules in the lattice.

Electrochemistry

Table 5 summarizes the electrochemical data obtained in CH_3CN for the series of complexes **1**–**12**. Since complex **9** undergoes an immediate solvolysis in CH_3CN, its electrochemical behaviour was examined in an acetone–water mixture (95/5, v/v). All the complexes studied display a reversible metal-centered process and two reversible ligand-centered processes corresponding to the formation of radical anions, as electrons are added to the π* orbitals of the ligands. By comparison with ligand reduction processes occuring in [Ru(phen)$_3$]$^{2+}$ (−1.41 V), [Ru(terpy)$_2$]$^{2+}$ (−1.29 and −1.54 V) and ESR measurements performed on [Ru(terpy)(bpy)(py)]$^{2+}$,[22] it can be assumed that the first one-electron reduction concerns the terpyridine and the second concerns the phenanthroline. The redox potential of the Ru(III/II) couple is highly dependent on the σ-donor and π-acceptor properties of the coordinated ligands. In this series, terpy and phen are the better π-acceptor ligands, so the redox potential of the metal is mainly influenced by the σ-donating ability of the sixth monodentate ligand.[23] From Table 5 it is clear that good σ-donor ligands such as Cl^- in **1** and

Table 5 Cyclic voltammetry data of the complexes **1**–**12** in CH_3CN, except **9** which is in acetone–water (95/5, v/v); ($Bu^n_4NPF_6$ 0.1 M, v = 100 mV s^{-1})

	$E_{1/2}$/V *vs.* SCE ($\|E_{pa} - E_{pc}\|$/mV)				
Complex	Ru(III/II)	$mqt^{+/0}$	terpy/terpy$^-$	$mqt^{0/-1}$	phen/phen$^-$
1	0.78 (70)		−1.44 (80)		−1.59 (80)
2	1.27 (60)		−1.31 (60)		−1.60 (60)
3	1.05 (60)		−1.40 (60)		−1.70 (70)
4	1.23 (70)		−1.26 (60)		−1.59 (70)
5	1.23 (70)		−1.26 (60)		−1.59 (70)
6	1.05 (60)		−1.30 (70)		−1.62 (80)
7[b]	1.28 (60); 1.05 (150)		−1.32 (90)		−1.60 (60)
8	1.26 (80)	−0.77 (60)	−1.26 (60)	−1.44 (70)	−1.59 (70)
9	0.89 (100)[a]		−1.24 (70)		−1.42 (100)
10	1.20 (60)		−1.27 (60)		−1.59 (60)
11	0.79 (60)		−1.44 (70)		−1.59 (80)
12	1.27 (60)		−1.28 (70)		−1.58 (80)

[a] Two-electron redox process. [b] Additional reduction peak at 0.66 V.

dimethylaminopyridine in **6** shift the redox potential of the metal to much less positive values than those observed for **4**.

Isoquinoline and 3,5-dimethylpyridine have σ-donor properties similar to pyridine, and therefore have little effect on the Ru(III/II) process, while this process in **8**, in which the ligand is positively charged, occurs at a slightly more positive potential. For this complex, four reversible reduction waves are observed, at −0.77, −1.26, −1.44, −1.59 V. The first corresponds to the reduction of the monocationic mqt^+ ligand giving $[Ru(terpy)(phen)(mqt^{+\bullet})]^{2+}$. The reduction of this species, which occurs on the terpy ligand giving $[Ru(terpy^{-\bullet})(phen)(mqt^{+\bullet})]^+$, is followed by a second process based on the neutral mqt ligand, which gives $[Ru(terpy^{-\bullet})(phen)(mqt^{-\bullet})]$, and the final process occurs on the phen ligand giving $[Ru(terpy^{-\bullet})(phen^{-\bullet})(mqt^{-\bullet})]$–. The two additional waves can be assigned to the reduction of the alkylated pyridine unit since the free *N*-methyl-4,4′-bipyridinium salt undergoes reduction processes at −0.92 and −1.62 V,[24] which are shifted to more positive potentials by approximately 200 mV on coordination to Ru(II).[19] The electrochemical behavior of **7** is more complicated since two reversible anodic processes are observed at 1.05 and 1.28 V along with a third process at 0.66 V, which is present only in the return wave. The process at 1.05 V is thought to be that of **7**, which undergoes ligand dissociation on oxidation to give **2**, the Ru(III/II) process of which occurs at 1.28 V. The process at 0.66 V is ascribed to the reduction of the dissociated ptz radical cation: this process is present even when the potential of the CV is switched at 1.2 V, demonstrating it is not a product of the process at 1.28 V. This electrochemically induced ligand dissociation is not observed for any of the other complexes in the series, but has been documented in the analogous complex $[Ru(terpy)(bpy)(ptz)]^{2+}$.[18] Complex **9** shows a single redox wave at surprisingly high potential (0.89 V) corresponding to a two-electron redox process. As indicated by its broad shape (ΔE_p = 100 mV) this wave is probably due to two very close one-electron processes Ru(III/II) and Ru(IV/III) associated with proton-coupled reactions such as that of $[Ru(tpy)(bpz)(H_2O)]^{2+}$ which is thought to undergo a two-proton, two-electron oxidative process to give $[Ru(tpy)(bpz)(O)]^{2+}$.[15] Such behaviour has also been observed in other ruthenium polypyridine aqua complexes[15,20,25] in which the Ru(III) oxidation state is unstable with respect to disproportionation in the considered medium.This observation is in accordance with the electrochemical behavior of $[Ru(terpy)(phen)(H_2O)]^{2+}$, which posesses the smallest $\Delta E_{1/2}$ value ($\Delta E_{1/2} = E°(Ru^{IV/III}) - E°(Ru^{III/II})$) of the 22 complexes of this type.[26]

Spectroscopic properties

The absorption spectra for all the complexes are dominated by intense ligand centered (π–π*) transition bands in the ultraviolet region while unresolved overlapping metal-to-ligand charge transfer bands (^{1}MLCT) are observed in the visible region (Table 6 and Fig. 2).

Table 6 Electronic spectral data of the complexes **1**–**12** in CH_3CN, except **9** which is in CH_2Cl_2

Complex	Absorption λ_{max}/nm ($10^{-3}\varepsilon$/$M^{-1}cm^{-1}$)[a]	Emission λ_{max}/nm[b]
1	380 (3.05), 439 (6.04), 502 (9.43)	710
2	398sh (7.37), 455 (11.51)	–
3	357 (3.36), 417sh (6.87), 486 (11.73)	630
4	411 (7.74), 467 (9.26)	640
5	370 (7.55), 416 (11.79), 472 (9.90)	640
6	364 (5.42), 416 (7.82), 474 (8.51)	670
7	413 (6.93), 461sh (6.14)	–
8	441 (10.90), 475sh (8.84)	–
9	314 (35.5), 486 (13.7)	–
10	395sh (6.8), 468sh (10.6), 487 (11.4)	640
11	316 (25.5), 510 (11.7)	727
12	310 (39.9), 464 (17.8)	614

[a] 293 K. [b] Deoxygenated solvent, $\lambda_{ex} = \lambda_{max}$ of the MLCT band, 293 K.

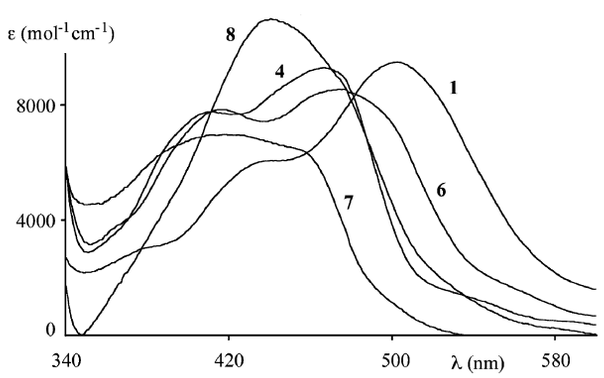

Fig. 2 Visible electronic spectra of **1**, **4**, **6**, **7** and **8** in CH_3CN.

Since the energy of the π* orbitals of the terpy and phen acceptor ligands is not affected by minor changes in the ligand field around the metal, the wavelength of the MLCT bands is determined by the energy of the metal $d(t_{2g})$ orbitals, which is modified by the donor or acceptor nature of ligand L. As the σ-donor ability of the ligand increases, the absorption maximum wavelength (nm) of the complexes with the terpy ligand shifts to lower energy following the series: **8** (441) < **4** (467) < **5** (472) < **6** (474) < **1** (502). In the case of **5** the most intense absorption occurs at 416 nm; however, this can be assigned to the Ru–isoquinoline absorption since it occurs in the same position as the Ru–pyridine transition (413 nm) but with greater intensity due to increased conjugation. A ligand such as CH_3CN, which is a strong π-acceptor and weak σ-donor, lowers the energy of the metal $d(t_{2g})$ orbitals compared to pyridine,

Table 7 Crystallographic data for **1**–**5**

	1	**2**	**3**	**4**	**5**
Formula	$C_{31}H_{25}ClF_6N_7PRu$	$C_{33}H_{28}F_{12}N_8P_2Ru$	$C_{28}H_{21}F_6N_6OPRu$	$C_{38}H_{30}F_{12}N_6P_2Ru$	$C_{79}H_{60}Cl_2F_{24}N_{12}P_4Ru_2$
M_r	777.08	927.64	703.55	961.70	2030.34
Crystal system	Triclinic	Monoclinic	Triclinic	Monoclinic	Monoclinic
Space group	$P\bar{1}$	$P2_1/c$	$P\bar{1}$	$P2_1/c$	$C2/c$
a/Å	8.8775(4)	8.7526(3)	8.6848(3)	15.3374(5)	14.0923(4)
b/Å	12.0354(5)	11.5332(2)	10.3229(7)	19.8829(8)	21.9960(8)
c/Å	15.3203(6)	36.851(1)	16.632(1)	12.9446(4)	25.6543(6)
α/°	80.973(8)		79.267(5)		
β/°	80.067(8)	92.216(5)	77.266(5)	105.241(5)	99.395(5)
γ/°	85.708(8)		68.952(5)		
V/Å^3	1590.5(1)	3717.1(3)	1347.9(1)	3808.6(5)	7845.5(4)
Z	2	4	2	4	4
Color	Red	Orange	Orange	Red	Red
D_c/g cm^{-3}	1.62	1.66	1.73	1.68	1.72
μ/mm^{-1}	0.697	0.606	0.719	0.594	0.647
T/K	173	173	173	173	173
R^a	0.038	0.041	0.032	0.043	0.052
$R_w{}^b$	0.051	0.050	0.038	0.061	0.072

^{a} $R = \Sigma||F_o| - |F_c||/|F_o|$. ^{b} $R_w = [\Sigma w(|F_o| - |F_c|)^2/\Sigma w(|F_o|^2)]^{1/2}$.

causing a shift in the MLCT maximum to shorter wavelength (455 nm). In the case of CN^-, which is a strong π-acceptor but also a stronger σ-donor, a bathochromic shift is also observed (486 nm). According to literature data the complexes of the type Ru(terpy)(bpy)L^{2+} are generally weak emitters.[9a,13a] As indicated in Table 6, emission data shows that some of the complexes are weakly emissive at room temperature in CH_3CN, that the emission is stronger when L is dimethylaminopyridine, but that luminescence is quenched in **7**, **8** and **9**, which suggests that the energy difference between the ^{3}MC and the ^{3}MLCT states is small enough for thermal deactivation to proceed by this pathway.

Photochemical reactivity

The photochemistry of these new ruthenium complexes was examined both for synthetic utility and as model reactions in the design of molecular machines triggered by a photonic signal. The irradiation of **1** for 5 h in CH_3CN–H_2O affords **2** in 87% yield. Synthesis of complexes **4**–**8** was carried out by dissolving **2** in deoxygenated acetone to which ten equivalents excess of the ligand L was added. The reaction mixture was irradiated and the solution stirred under argon while the progress of the reaction was monitored by thin layer chomatography. After purification by column chromatography, the products were isolated as their hexafluorophosphate salts in 78–82% yields. On irradiation of **4**, **6**, **7** and **10** in acetonitrile, photoinduced exchange of ligand L for CH_3CN occurs. The rates of completion of this exchange process vary dramatically depending on ligand L. When L is phenothiazine the process is finished after 5 min, while when L is dimethylaminopyridine the exchange has not reached completion after 16 h. Photolabilisation occurs when the excited complex undergoes a thermally assisted transition from the ^{3}MLCT to the ^{3}MC excited state; this is also the pathway which leads to luminescence quenching in the complex. Hence, the complex which luminesces with the greatest intensity, **6**, is the complex for which the photolabilisation process is the slowest. This type of ligand interchange also occurs efficiently and very selectively with other types of ligands such as thioethers, ethers, pyridines, sulfoxides, nitriles and amides.

Conclusion

A series of ruthenium complexes of formula [Ru(terpy)(phen)(L)]$^{n+}$ has been prepared and fully characterized. The electrochemical and photophysical properties of the metal complex can be altered depending on the nature of the ligand L. The synthetic procedures detailed in this study are among the few examples of photoexchange being used preparatively to give high yields of the desired compounds. Their success opens up new routes to efficient synthesis of such complexes and the high yields of these processes suggest their use in systems capable of molecular motion.

Experimental

Single crystal X-ray diffraction experiments were carried out using Kappa CCD and graphite-monochromated Mo-Kα radiation (λ = 0.71073 Å). For all computations, the MolEN package was used[27a] and structures were drawn using ORTEP.[27b] Crystal data and details of data collection for complexes **1**–**10** are provided in Tables 7 and 8.

CCDC reference numbers 218272–218280 and 218935.

See http://www.rsc.org/suppdata/dt/b3/b310198c/ for crystallographic data in CIF or other electronic format.

^{1}H NMR spectra were acquired on either a Bruker WP200 SY (200 MHz) or a Bruker AM 400 (400 MHz) spectrometer, using the deuterated solvent as the lock and residual solvent as the internal reference. Mass spectra were obtained by using a VG ZAB-HF (FAB) spectrometer or a VG-BIOQ triple quadrupole, positive mode (ES-MS). Photoirradiation was performed in a quartz UV cell (l = 1.0 cm) or in a NMR tube (ϕ = 5.0 mm) using a Hanimex slide projector (250 W halogen lamp, λ > 400 nm). Electrochemical experiments were performed using an EG&G PAR model 273A potentiostat with a standard three-electrode configuration. Cyclic voltammetry was carried out in MeCN solution, using Bu_4NPF_6 as supporting electrolyte, a Pt working electrode, a Pt counter-electrode, and SCE as reference. The typical sweep rate was 100 mV s^{-1}, and the window used was from −2.0 to +1.7 V. Absorption spectra were recorded with a Kontron Uvikon 860. Emission spectra were obtained with a SLM Aminco-Bauman Series 2 spectrofluorimeter.

Chemicals: The ligand terpy* was prepared following literature procedures.[28]

Ru(terpy*)Cl_3: 4-(3,5-di-*tert*-butyl)phenyl-2,2′;6′,2″-terpyridine (201 mg, 0.479 mmol) and one equivalent of $RuCl_3 \cdot 3H_2O$ (125 mg, 0.478 mmol) were dissolved in ethanol (30 cm^3). The solution was heated to reflux for 1 h, cooled and the precipitate isolated by filtration. The orange solid was washed twice with ethanol, once with water, once with diethyl ether and air dried (Yield 299 mg, 99.5%). FAB-MS *m*/*z* (calc.): 628.1 (628.1, [M]$^+$), 593.1 (593.1, [M − Cl]$^+$), 558.1 (558.1, [M − 2 Cl]$^+$), 523.2 (523.2, [M − 3 Cl]$^+$).

1: [Ru(terpy)(phen)Cl][PF_6]. A mixture of Ru(terpy)Cl_3 (500 mg, 1.13 mmol), 1,10-phenanthroline (215 mg, 1.19

Table 8 Crystallographic data for **6**–**10**

	6	**7**	**8**	**9**	**10**
Formula	$C_{38}H_{35}F_{12}N_9P_2Ru$	$C_{88}H_{74}F_{24}N_{12}O_2P_4Ru_2S_2$	$C_{164}H_{140}F_{72}N_{34}OP_{12}Ru_4$	$C_{97}H_{112}F_{24}N_{10}O_7P_4Ru_2$	$C_{55}H_{64}F_{12}N_6O_2P_2Ru$
M_r	1008.76	2177.78	4747.02	2312.03	1232.16
Crystal system	Triclinic	Triclinic	Triclinic	Hexagonal	Monoclinic
Space group	$P\bar{1}$	$P\bar{1}$	$P\bar{1}$	$P322_1$	$C2/c$
a/Å	9.0753(2)	10.2143(3)	17.0076(5)	13.5432(1)	23.7601(2)
b/Å	11.5163(4)	12.4444(5)	17.7093(6)	13.5432(1)	13.1662(1)
c/Å	20.6798(6)	19.6448(8)	18.7337(5)	50.1170(3)	37.2176(4)
α/°	76.071(5)	97.540(5)	62.319(5)	90	
β/°	88.935(5)	94.916(5)	85.332(5)	90	97.638(5)
γ/°	89.917(5)	111.387(5)	71.423(5)	120	
V/Å^3	2097.4(1)	2280.8(1)	4721.4(2)	7960.8(1)	11539.5(2)
Z	2	1	1	3	8
Color	Red	Orange	Red	Red	Red
D_c/g cm^{-3}	1.60	1.59	1.67	1.45	1.42
μ/mm^{-1}	0.545	0.551	0.548	0.443	0.411
T/K	173	173	173	173	173
R^a	0.038	0.076	0.084	0.073	0.066
R_w [b]	0.049	0.092	0.104	0.091	0.079

[a] $R = \Sigma||F_o| - |F_c||/|F_o|$. [b] $R_w = [\Sigma w(|F_o| - |F_c|)^2/\Sigma w(|F_o|^2)]^{1/2}$.

mmol), lithium chloride (265 mg, 6.24 mmol) and triethylamine (1 cm^3) was heated to reflux in EtOH–H_2O (3 : 1, 50 cm^3) for 4 h. Half of the solvent was removed *in vacuo*, and the brown solution was poured into a solution of aqueous KPF_6 (100 cm^3). The precipitate was collected by filtration, the solvent removed and the residue separated by column chromatography (silica: MeCN–H_2O–sat.$KNO_{3(aq)}$, 44 : 2 : 1). The major fraction was collected, reduced in volume, and precipitated by the addition of a solution of aqueous KPF_6. The precipitate was collected by filtration over Celite, redissolved in MeCN and the solvent removed *in vacuo*, giving a brown powder (323 mg, 41%). ^{1}H NMR (300 MHz, CD_3CN): δ 10.43 (H, dd, J 5.2, 1.2 Hz, H^{P2}), 8.81 (H, dd, J 8.1 Hz, H^{P4}), 8.53 (2H, d, J 8.1 Hz, H^{B3}), 8.38 (2H, ddd, J 8.1 Hz, H^{A3}), 8.31 (H, dd, H^{P3}), 8.30 (H, AB, J 8.9 Hz, H^{P5}), 8.22 (H, dd, J 8.1, 1.2 Hz, H^{P9}), 8.13 (H, t, H^{B4}), 8.02 (H, AB, H^{P6}), 7.83 (2H, ddd, J 1.7 Hz, H^{A4}), 7.65 (H, dd, J 5.4 Hz, H^{P7}), 7.51 (2H, dm, H^{A6}), 7.28 (H, dd, H^{P8}), 7.12 (2H, ddd, J 7.6, 5.4, 1.2, H^{A5}). Crystals of (**1**)$(PF_6)\cdot 2CH_3CN$ were obtained by vapour diffusion, in the dark, of diisopropyl ether into a solution of the product in CH_3CN.

2: [Ru(terpy)(phen)(CH_3CN)][PF_6]$_2$: *thermal preparation*. A mixture of [Ru(terpy)(phen)Cl][PF_6] (250 mg, 0.36 mmol) and $AgBF_4$ (116 mg, 0.60 mmol) was heated to reflux in CH_3CN–H_2O (4 : 1, 250 cm^3) for 3 h. The solution was filtered hot through Celite to remove AgCl then half the solvent was removed *in vacuo*. On pouring the solution into a solution of aqueous KPF_6 (200 mL) an orange solid precipitated which was collected by filtration on Celite. This solid was purified by column chromatography (silica: MeCN–H_2O–sat. $KNO_{3(aq)}$, 44 : 2 : 1). The major, orange fraction was collected, and the complex was precipitated by the addition of a solution of aqueous KPF_6. Following filtration the product was dried *in vacuo* and isolated as an orange powder (256 mg, 84%). ^{1}H NMR (400 MHz, CD_3CN): δ 9.97 (H, dd, J 1.2 Hz, H^{P2}), 8.93 (H, dd, J 8.2, 1.2 Hz, H^{P4}), 8.63 (2H, d, J 8.2 Hz, H^{B3}), 8.46 (2H, ddd, J 8.2, 1.3, 0.8 Hz, H^{A3}), 8.41 (H, dd, J 8.2, H^{P9}), 8.37–8.41 (2H, m, $H^{P5,B4}$), 8.36 (H, dd, J 8.2, 5.3 Hz, H^{P3}), 8.17 (H, d, J 9.0, H^{P6}), 7.99 (2H, ddd, J 8.2, 1.6 Hz, H^{A4}), 7.67 (H, dd, J 5.3, 1.3 Hz, H^{P7}), 7.57 (2H, ddd, J 5.5, 1.6, 0.8, H^{A6}), 7.46 (H, dd, J 8.2, 5.3, H^{P8}), 7.25 (2H, ddd, J 7.6, 5.5, 1.3, H^{A5}), 2.14 (3H, s, CH_3CN). FAB-MS: m/z (calc.) 701.0 (700.6, [M − PF_6]$^+$), 555.0 (555.6, [M − 2PF_6]$^+$), 515.0 (514.6, [Ru(terpy)(bpy)]$^+$). Crystals of (**2**)$(PF_6)_2\cdot 2CH_3CN$ were obtained by vapour diffusion, in the dark, of diisopropyl ether into a solution of the product in CH_3CN.

Photochemical preparation. A solution of [Ru(terpy)(phen)Cl][PF_6] (50 mg, 0.072 mmol) in degassed CH_3CN (20 cm^3) and H_2O (10 cm^3) was irradiated with white light from a slide projector for 5 h. The solvent was then removed under vacuum followed by addition of water (10 cm^3) and then a solution of aqueous KPF_6 (10 cm^3) were added resulting in the precipitation of an orange solid, which was collected by filtration on Celite. This solid was purified by column chromatography (silica: MeCN–H_2O–sat. $KNO_{3(aq)}$, 44 : 2 : 1). The major, orange fraction was collected, and the complex was precipitated by the addition of a solution of aqueous KPF_6. Following filtration, the product was dried *in vacuo* and isolated as an orange powder (53 mg, 87%).

3: [Ru(terpy)(phen)(CN)][PF_6]. A second product with a higher R_f value was also isolated in the chromatographic separation from **2** prepared thermally. The yellow solid was identified as [Ru(terpy)(phen)(CN)][PF_6]. ^{1}H NMR (400 MHz, CD_3CN): δ 10.34 (H, d 4.4 Hz, H^{P2}), 8.78 (H, d, J 8.4 Hz, H^{P4}), 8.52 (2H, d, J 7.9 Hz, H^{B3}), 8.37 (3H, dm, $H^{A3,P9}$), 8.28 (H, AB, J 8.8, H^{P5}), 8.22 (H, dm, H^{P3}), 8.21 (H, t, H^{B4}), 8.11 (H, AB, H^{P6}), 7.88 (2H, ddd, J 7.6 Hz, H^{A4}), 7.63 (H, dd, J 5.2, 1.5 Hz, H^{P7}), 7.55 (2H, dm, J 5.4, H^{A6}), 7.43 (H, dd, J 8.4, 5.2, H^{P8}), 7.14 (2H, ddd, J 1.5 Hz, H^{A5}). FAB-MS: m/z (calc.) 541.0 (540.6, [M − 2PF_6]), 514.0 (514.6, [Ru(terpy)(phen)]$^+$). Crystals of (**3**)$(PF_6)\cdot H_2O$ were obtained by vapour diffusion, in the dark, of diisopropyl ether into a solution of the product in CH_3CN

4: [Ru(terpy)(phen)(py)][PF_6]$_2$. A solution of [Ru(terpy)-(phen)(CH_3CN)][PF_6]$_2$ (20 mg, 0.024 mmol) in degassed pyridine (20 cm^3) was irradiated with white light from a slide projector for 3 h. The solvent was then removed under vacuum, and water (10 cm^3) and then a solution of aqueous KPF_6 (10 cm^3) were added resulting in the precipitation of an orange solid which was collected by filtration on Celite to give dark red crystals (18 mg, 86%). ^{1}H NMR (400 MHz, CD_3CN): δ 9.11 (H, dd, J 5.2, 1.3 Hz, H^{P2}), 8.90 (H, dd, J 8.4 Hz, H^{P4}), 8.59 (2H, d, J 8.2 Hz, H^{B3}), 8.47 (2H, ddd, J 8.2, 1.3, 0.8 Hz, H^{A3}), 8.42 (H, dd, J 8.4, 1.3 Hz, H^{P9}), 8.38 (H, AB, J 9.0, H^{P5}), 8.28 (H, t, H^{B4}), 8.22 (H, d, H^{P3}), 8.20 (H, AB, H^{P6}), 8.01 (2H, ddd, J 9.2, 1.6 Hz, H^{A4}), 7.88–7.86 (3H, m, H^{py}), 7.67 (H, dd, J 5.3 Hz, H^{P7}), 7.64 (2H, ddd, J 5.5, H^{A6}), 7.45 (H, dd, H^{P8}), 7.31–7.26 (4H, m, $H^{A5,py}$). FAB-MS: m/z (calc.) 739.0 (738.7, [M − PF_6]$^+$). Crystals of (**4**)$(PF_6)_2\cdot C_6H_6$ were obtained by vapour diffusion, in the dark, of benzene into a solution of the product in CH_3CN.

5: [Ru(terpy)(phen)(iq)][PF_6]$_2$. A mixture of [Ru(terpy)-(phen)(CH_3CN)][PF_6]$_2$ (20 mg, 0.024 mmol) and isoquinoline (35 mg, 0.271 mmol) in degassed acetone (5 cm^3) was irradiated with white light from a slide projector for 7 h under argon. Following purification of the crude product by column chromatography (silica: MeCN–H_2O–sat. $KNO_{3(aq)}$, 44 : 2 : 1), the

major orange fraction was collected, and the complex was precipitated by the addition of a solution of aqueous KPF_6. The precipitate was collected on Celite, redissolved in CH_3CN and dried under vacuum giving an orange powder (18 mg, 82%). ^1H NMR (500 MHz, CD_3CN): δ 9.15 (H, dd, J 5.2, 1.3 Hz, H^{P2}), 8.88 (H, dd, J 8.3, 1.3 Hz, H^{P4}), 8.58 (2H, d, J 8.2 Hz, H^{B3}), 8.49 (H, d, J 0.7 Hz, H^{iq2}), 8.46 (2H, ddd, J 8.1 Hz, H^{A3}), 8.41 (H, dd, H^{P9}); 8.36 (H, AB, J 8.9 Hz, H^{P5}), 8.25 (H, t, J 8.1 Hz, H^{B4}), 8.19 (H, AB, H^{P6}), 8.16 (H, dd, J 8.3, 5.2 Hz H^{P3}), 8.00 (2H, ddd, J 9.2, 6.7, 1.5 Hz, H^{A4}), 7.82 (H, t, J 7.5 Hz, H^{iq}), 7.66–7.71 (6H, m, $H^{P7,A6,iq}$), 7.44 (H, dd, J 8.2, 5.3, H^{P8}), 7.29 (2H, ddd, H^{A5}). FAB-MS: m/z (calc.) 789.3 (788.7, $[M - PF_6]^+$), 644.3 (643.7, $[M - 2PF_6]^+$), 515.3 (514.7, $[Ru(terpy)(phen)]^+$), 322.2 (321.9, $[M - 2PF_6]^{2+}$) Crystals of $(\mathbf{5})_2(PF_6)_4 \cdot C_6H_6 \cdot CH_2Cl_2$ were obtained by vapour diffusion, in the dark, of benzene into a solution of the product in CH_2Cl_2.

6: $[Ru(terpy)(phen)(dmap)][PF_6]_2$. The same procedure as described for **5** led to **6** after 16 h of irradiation, in 96% yield. ^1H NMR (500 MHz, CD_3CN): δ 9.12 (H, dd, J 5.2, 1.3 Hz, H^{P2}), 8.86 (H, dd, J 8.3 Hz, H^{P4}), 8.55 (2H, d, J 8.2 Hz, H^{B3}), 8.43 (2H, ddd, J 8.1, 3.4 Hz, H^{A3}), 8.33–8.36 (2H, m, $H^{P9,P5}$), 8.18–8.22 (2H, m, $H^{P3,B4}$), 8.15 (H, AB, J 8.9, H^{P6}), 7.95 (2H, ddd, J 6.2, 1.5 Hz, H^{A4}), 7.62 (H, dd, J 4.2 Hz, H^{P7}), 7.59 (2H, dm, J 5.5, H^{A6}), 7.38 (H, dd, J 8.3 Hz, H^{P8}), 7.23 (2H, ddd, H^{A5}), 7.16 (2H, AB, J 7.4 Hz, H^{dmap}), 6.36 (2H, AB, H^{dmap}), 2.90 (6H, s, H^{CH_3}). FAB-MS: m/z (calc.) 782.1 (781.3, $[M - PF_6]^+$), 636.8 (637.2, $[M - 2PF_6]^+$), 515.1 (514.6, $[Ru(terpy)(phen)]^+$), 318.8 (318.4, $[M - 2PF_6]^{2+}$). Crystals of $(\mathbf{6})(PF_6)_2 \cdot 2CH_3CN$ were obtained by vapour diffusion, in the dark, of diisopropyl ether into a solution of the product in CH_3CN.

7: $[Ru(terpy)(phen)(ptz)][PF_6]_2$. The same procedure as described for **5** led to **7** after 41 h of irradiation, in 78% yield. ^1H NMR (400 MHz, CD_3CN): δ 10.76 (H, dd, H^{P2}), 8.95 (H, dd, H^{P4}), 8.49 (H, dd, J 8.3, 5.3 Hz, H^{P3}), 8.40 (H, dd, J 8.1, 1.2 Hz, H^{P9}), 8.34 (H, AB, J 8.9 Hz, H^{P5}), 8.32–8.24 (3H, m, $H^{B4,B3}$), 8.14 (H, AB, H^{P6}), 7.90 (2H, d, H^{A3}), 7.72 (2H, ddd, J 9.2, 7.4, 1.5 Hz, H^{A4}), 7.47 (H, dd, J 5.2, 1.2 Hz, H^{P7}), 7.40 (H, dd, H^{P8}), 7.34 (2H, dm, J 5.3, H^{A6}), 7.15 (H, s, $H^{ptz\text{-}NH}$), 7.00 (2H, ddd, J 8.3, 7.3, H^{ptz}), 6.95 (2H, ddd, J 7.4, 5.3, 1.3 Hz, H^{A5}), 6.52 (2H, dd, J 7.8, 1.3, H^{ptz}), 6.42–6.37 (4H, m, H^{ptz}), 6.52 (2H, dd, J 7.8, 1.3, H^{ptz}). FAB-MS: m/z (calc.) 859.3 (858.9, $[M - PF_6]^+$), 713.2 (713.9, $[M - 2PF_6]^+$), 515.2 (514.7, $[Ru(terpy)(phen)]^+$). Crystals of $(\mathbf{7})_2(PF_6)_4 \cdot CH_3OH \cdot C_8H_{10}$ were obtained by vapour diffusion, in the dark, of xylene into a solution of the product in methanol over three months.

8: $[Ru(terpy)(phen)(mqt)][PF_6]_3$. The same procedure as described for **5** led to **8** after 26 h of irradiation, in 80% yield. ^1H NMR (400 MHz, CD_3CN): δ 9.12 (H, dd, J 5.3, 1.3 Hz, H^{P2}), 8.99 (H, dd, J 8.3 Hz,H^{P4}), 8.68 (2H, d, J 6.8, H^{mqt}), 8.59 (2H, d, J 8.1 Hz, H^{B3}), 8.46 (2H, dm, J 8.0 Hz, H^{A3}), 8.40 (H, dd, J 8.3, 1.3 Hz, H^{P9}), 8.36 (H, AB, J 8.8 Hz, H^{P5}), 8.29 (H, t, J 8.1 Hz, H^{B4}), 8.20 (H, dd, H^{P3}), 8.18 (H, AB, H^{P6}), 8.16 (2H, d, J 7.0, H^{mqt}), 8.08 (2H, dd, J 5.4, 1.5, H^{mqt}), 8.00 (2H, ddd, J 9.3, 7.4, 1.5 Hz, H^{A4}), 7.65–7.61 (5H, m, $H^{P7,A6,mqt}$), 7.44 (H, dd, J 5.3 Hz, H^{P8}), 7.28 (2H, dd, J 7.4, 5.5 H^{A5}), 4.31 (3H, s, CH_3). FAB-MS: m/z (calc.) 976.3 (975.8, $[M - PF_6]^+$), 831.3 (830.8, $[M - 2PF_6]^+$), 515.2 (514.7, $[Ru(terpy)(phen)]^+$). Crystals of $(\mathbf{8})_4(PF_6)_{12} \cdot 6CH_3CN \cdot H_2O$ were obtained by vapour diffusion, in the dark, of diisopropyl ether into a solution of the product in CH_3CN.

9: $[Ru(terpy^*)(phen)(H_2O)][PF_6]_2$: $[Ru(terpy^*)(phen)Cl][PF_6]$ (113 mg, 0.128 mmol) and $AgBF_4$ (10 eq, 1.28 mmol) were dissolved in an acetone–water mixture (3 : 2, 100 cm^3). The solution was degassed and heated at reflux under argon for 3 h. AgCl was filtered over Celite, water and an aqueous solution of KPF_6 (50 cm^3) were added and acetone was evaporated. The red solid was isolated by filtration and washed with water (89 mg, 69%). ^1H NMR (300 MHz, CD_2Cl_2): δ 9.94 (H, d, J 4.9 Hz, H^{P2}); 8.82 (H, d, J 8.1 Hz, H^{P4}); 8.57 (2H, s, H^{B3}); 8.41 (2H, dd, J 7.4, 0.9 Hz, H^{A3}); 8.37 (H, dd, J 8.1 Hz, 4.9 Hz, H^{P3}); 8.29 (H, d, J 8.9 Hz, H^{P5}); 8.17 (H, d, J 8.1 Hz, H^{P7}); 8.06 (H, d, J 8.9 Hz, H^{P6}); 7.90 (2H, td, J 7.4 Hz, H^{A4}); 7.79 (2H, d, J 1.8 Hz, H^{C2}); 7.73 (H, t, J 1.8 Hz, H^{C4}); 7.64 (H, d, J 5.0 Hz, H^{P9}); 7.53 (2H, d, J 5.3 Hz, H^{A6}); 7.42 (H, dd, J 8.1, 5.0 Hz, H^{P8}); 7.25 (2H, m, H^{A5}); 1.50 (18H, s, H^{tBu}). ES-MS m/z (calc.): 722.2 (721.2, $[M - 2PF_6 + H]^+$); 848.2 (848.2, $[M - H_2O - PF_6]^+$); 380.5 (380.6, $[M - 2PF_6 - H_2O + \text{acetone}]^{2+}$). Recrystallisation by vapour diffusion in the dark, of diisopropyl ether into a solution of the product in acetone yielded crystals of $(\mathbf{9})_2(PF_6)_4 \cdot 5C_3H_6O$ suitable for X-ray analysis.

10: $[Ru(terpy^*)(phen)(lut)][PF_6]_2$: $[Ru(terpy^*)(phen)(CH_3CN)][PF_6]_2$ (24.5 mg, 0.024 mmol) was dissolved in 3,5-lutidine (5 cm^3). The solution was degassed and heated to reflux under argon for 2 h. The lutidine was removed under vacuum, acetone (1 cm^3) and an aqueous solution of KPF_6 (10 cm^3) were added, acetone was evaporated and the solid was filtered, washed with water, Et_2O and vacuum dried (Yield 23 mg, 88%). ^1H NMR (400 MHz, acetone-d_6): δ 9.39 (H, dd, J 5.4, 1.2 Hz, H^{P2}); 9.18 (2H, s, H^{B3}); 9.05 (H, dd, J 8.2, 1.2 Hz, H^{P4}); 8.90 (2H, m, J 7.8 Hz, H^{A3}); 8.57 (H, dd, J 8.2, 1.2 Hz, H^{P7}); 8.50 (H, d, J 8.8 Hz, H^{P5}); 8.37 (H, dd, J 8.2, 5.4 Hz, H^{P3}); 8.32 (H, d, J 8.8 Hz, H^{P6}); 8.15 (2H, td, J 7.8, 1.5 Hz, H^{A4}); 8.08 (H, dd, J 5.3, 1.2 Hz, H^{P9}); 8.04 (2H, d, J 1.8 Hz, H^{C2}); 8.01 (2H, dm, J 4.7 Hz, H^{A6}); 7.78 (3H, $H^{C4,lut2}$); 7.62–7.58 (2H, J 8.2, 5.3 Hz, $H^{P8,lut4}$); 7.44 (2H, m, H^{A5}); 2.14 and 2.14 (6H, 2s, $H^{lut\text{-}CH3}$); 1.49 (18H, s, H^{tBu}). ES-MS m/z (calc.): 955.3 (955.3, $[M - PF_6]^+$), 738.2 (738.2, $[M - 2PF_6 - 3,5\text{-lutidine} + Cl]^+$), 405.0 (405.2, $[M - 2PF_6]^{2+}$). Crystals of $(\mathbf{10})(PF_6)_2 \cdot C_3H_6O \cdot C_4H_{10}O$ were grown by slow vapour diffusion of Et_2O in an acetone solution of the complex.

11: $[Ru(terpy^*)(phen)Cl][PF_6]$: Crude $Ru(terpy^*)Cl_3$ (428 mg, 0.68 mmol), monoaqua-1,10-phenanthroline (1.04 eq, 0.708 mmol) and lithium chloride (5 eq., 3.41 mmol) and triethylamine (1.5 cm^3) were heated at reflux in a degassed mixture of water (40 cm^3) and ethanol (120 cm^3) under argon for 4 h. A solution of saturated aqueous KPF_6 (40 cm^3) was added to the cooled dark reddish solution, the ethanol was evaporated and the violet precipitate filtered and washed twice with water and once with ether. Column chromatography on SiO_2 (eluent acetone–water–saturated KNO_3, 100 : 5 : 0.1) and vapour diffusion of diethyl ether into an acetone solution of the product yielded $[Ru(terpy^*)(phen)Cl][PF_6]$ (377 mg, 62%). ^1H NMR (400 MHz, acetone-d_6): δ 10.57 (H, dd, J 5.2,1.5 Hz, H^{P2}); 9.04 (2H, s, H^{B3}); 8.97 (H, dd, J 8.2, 1.5 Hz, H^{P4}); 8.75 (2H, d, J 8.0 Hz, H^{A3}); 8.45 (H, dd, J 5.2, 8.2 Hz, H^{P3}); 8.45 (H, d, J 8.9 Hz, H^{P5}); 8.40 (H, dt, J 8.1, 1.1 Hz, H^{P7}); 8.23 (H, d, J 8.9 Hz, H^{P6}); 8.04 (2H, d, J 1.7 Hz, H^{C2}); 8.03 (H, dd, J 5.4, 1.1 Hz, H^{P9}); 7.94 (2H, td, J 8.0, 1.5 Hz, H^{A4}); 7.75 (H, t, J 1.7Hz, H^{C4}); 7.69 (2H, d, J 5.5 Hz, H^{A6}); 7.47 (H, dd, J 5.4, 8.1 Hz, H^{P8}); 7.24 (2H, ddd, J 7.6, 5.5, 1.3 Hz, H^{A5}); 1.50 (18H, s, H^{tBu}). ES-MS m/z (calc.): 738.2 (738.2, $[M - PF_6]^+$).

12: $[Ru(terpy^*)(phen)(CH_3CN)][PF_6]_2$: $[Ru(terpy^*)(phen)Cl][PF_6]$ (199 mg, 0.226 mmol) and $AgBF_4$ (53.4 mg, 0.259 mmol) were dissolved in a mixture of water and acetonitrile (1 : 4, 60 cm^3). The degassed solution was heated to reflux under argon for 4.5 h. Silver chloride was removed by filtration over Celite, the volume of acetonitrile was reduced by evaporation and a solution of saturated aqueous KPF_6 (30 cm^3) was added. Evaporation of the remaining acetonitrile followed by filtration, washing with water and vacuum drying yielded $[Ru(terpy^*)(phen)(CH_3CN)][PF_6]_2$ quantitatively. ^1H NMR (300 MHz, acetone d_6): δ 10.28 (H, dd, J 5.2, 1.5 Hz, H^{P2}); 9.20 (2H, s, H^{B3}); 9.08 (H, dd, J 8.3, 1.5Hz, H^{P4}); 8.89 (2H, m, J 8.0 Hz, H^{A3}); 8.57 (H, dd, J 8.4, 1.2 Hz, H^{P7}); 8.50 (H, d, J 8.9 Hz, H^{P5}); 8.48 (H, dd, J 8.3, 5.2 Hz, H^{P3}); 8.29 (H, d, J 8.9 Hz, H^{P6}); 8.12 (2H, td, J 8.0, 1.5 Hz, H^{A4}); 8.09 (H, dd, J 5.3, 1.2 Hz, H^{P9}); 8.05 (2H, d, J 1.7 Hz, H^{C2}); 7.87 (2H, dm, J 5.4 Hz, H^{A6}); 7.81 (H, t, J 1.7 Hz, H^{C4}); 7.60 (H, dd, J 5.3, 8.4 Hz, H^{P8}); 7.38 (2H, ddd, J 5.4, 8.0, 1.2 Hz, H^{A5}); 2.42 (3H, s, H^{AN-CH3}); 1.50 (18H, s, H^{tBu}). ES-MS m/z (calc.): 889.3 (889.2, $[M - PF_6]^+$), 744.3 (744.3, $[M - 2PF_6]^+$), 371.9 (372.1, $[M - 2PF_6]^{2+}$).

Acknowledgements

We would like to thank the CNRS for financial support and the European Commission for Marie Curie Postdoctoral Fellowship (ERS). S. B. acknowledges support from the Region Alsace. We thank also Johnson Matthey Inc. for a loan of $RuCl_3$.

References

1 A. Juris, V. Balzani, F. Barigelletti, S. Campagna, P. Belser and A. Von Zelewsky, *Coord. Chem. Rev.*, 1988, **84**, 85–277; J.-P. Sauvage, J.-P. Collin, J.-C. Chambron, S. Guillerez, C. Coudret, V. Balzani, F. Barigelletti, L. De Cola and L. Flamigni, *Chem. Rev.*, 1994, **94**, 993–1019.

2 (*a*) A. P. De Silva, H. Q. N. Gunaratne, T. Guunlaugsson, A. J. M. Huxley, C. P. McCoy, J. T. Rademacher and T. E. Rice, *Chem Rev.*, 1997, **97**, 1515–1566; (*b*) M. H. Keefe, K. D. Benkstein and J. T. Hupp, *Coord. Chem. Rev.*, 2000, **205**, 201–228; (*c*) C. W. Rogers, Y. Zhang, B. O. Patrick, W. E. Jones and M. O. Wolf, *Inorg. Chem.*, 2002, **41**, 1162–1169.

3 S. Welter, K. Brunner, J. W. Hofstraat and L. De Cola, *Nature*, 2003, **421**, 54–57.

4 P. Belser, S. Bernhard, C. Blum, A. Beyeler, L. De Cola and V. Balzani, *Coord. Chem. Rev.*, 1999, **190–192**, 155–169.

5 (*a*) J. J. Rack, J. R. Winkler and H. B. Gray, *J. Am. Chem. Soc.*, 2001, **123**, 2432–2433; (*b*) M. K. Smith, J. A. Gibson, C. G. Young, J. A. Broomhead, P. C. Junk and F. R. Keene, *Eur. J. Inorg. Chem.*, 2000, 1365–1370; (*c*) B. Durham, S. R. Wilson, D. J. Hodgson and T. J. Meyer, *J. Am. Chem. Soc.*, 1980, **102**, 600–607.

6 (*a*) A. von Zelewsky and G. Gremaud, *Helv. Chim. Acta*, 1988, **71**, 1108–1115; (*b*) A.-C. Laemmel, J.-P. Collin and J.-P. Sauvage, *Eur. J. Inorg. Chem.*, 1999, 383–386; (*c*) E. Baranoff, J.-P. Collin, Y. Furusho, A.-C. Laemmel and J.-P. Sauvage, *Chem. Commun.*, 2000, 1935–1936.

7 (*a*) D. Pomeranc, D. Jouvenot, J.-C. Chambron, J.-P. Collin, V. Heitz and J.-P. Sauvage, *Chem. Eur. J.*, 2003, **9**, 4247–4254; (*b*) E. R. Schofield, J.-P. Collin, N. Gruber and J.-P. Sauvage, *Chem. Commun.*, 2003, 188–189.

8 (*a*) J.-P. Collin, A.-C. Laemmel and J.-P. Sauvage, *New J. Chem*, 2001, **25**, 22–24; (*b*) A.-C. Laemmel, J.-P. Collin and J.-P. Sauvage, *C.R. Acad. Sci. Paris*, 2000, **3**, 43–49.

9 (*a*) C. R. Hecker, P. E. Fanwick and D. R. MacMillin, *Inorg. Chem.*, 1991, **30**, 659–666; (*b*) H.-F. Suen, S. W. Wilson, M. Pomerantz and J. L. Walsh, *Inorg. Chem.*, 1989, **28**, 786–791.

10 (*a*) W. Weber and P. Ford, *Inorg. Chem.*, 1986, **25**, 1088–1092; (*b*) N. C. Fletcher and F. R. Keene, *J. Chem. Soc., Dalton Trans.*, 1998, 2293–2301; (*c*) D. A. Freedman, K. K. Evju, M. K. Pomije and K. R. Mann, *Inorg. Chem.*, 2001, **40**, 5711–5715.

11 (*a*) B. Durham, J. L. Walsh, C. L. Carter and T. J. Meyer, *Inorg. Chem.*, 1980, **19**, 860–865; (*b*) P. J. Steel, F. Lahousse, D. Lerner and C. Marzin, *Inorg. Chem.*, 1983, **22**, 1488–1493; (*c*) P. Bonneson, J. L. Walsh, W. T. Pennington, A. W. Cordes and B. Durham, *Inorg. Chem.*, 1983, **22**, 1761–1765.

12 (*a*) B. P. Sullivan, J. M. Calvert and T. J. Meyer, *Inorg. Chem.*, 1980, **19**, 1404–1047; (*b*) J. M. Calvert, R. H. Schmehl, B. P. Sullivan, J. S. Facci, T. J. Meyer and R. W. Murray, *Inorg. Chem.*, 1983, **22**, 2151–2162.

13 (*a*) S. C. Rasmussen, S. E. Ronco, D. A. Mlsna, M. A. Billadeau, W. T. Pennington, J. K. Lolis and J. D. Petersen, *Inorg. Chem.*, 1995, **34**, 821–829; (*b*) P. A. Adcock, F. R. Keene, R. S. Smythe and M. R. Snow, *Inorg. Chem.*, 1984, **23**, 2336–2343; (*c*) P. T. Gulyas, T. W. Hambley and P. A. Lay, *Aust. J. Chem.*, 1996, **49**, 527–532.

14 A. L. Spek, A. Gerli and J. Reedijk, *Acta Crystallogr., Sect. C*, 1994, **50**, 394–397.

15 A. Gerli, J. Reedijk, M. T. Lakin and A. L. Spek, *Inorg. Chem.*, 1995, **34**, 1836–1843.

16 F. Barigelletti, B. Ventura, J.-P. Collin, R. Kayhanian, P. Gavina and J.-P. Sauvage, *Eur. J. Inorg. Chem.*, 2000, 113–119.

17 D. J. Maloney and F. M. MacDonnell, *Acta Crystallogr., Sect. C*, 1999, **55**, 64–67.

18 R. Kroener, M. J. Heeg and E. Deutsch, *Inorg. Chem.*, 1988, **27**, 558–566.

19 B. J. Coe, M. C. Chamberlain, J. P. Essex-Lopresti, S. Gaines, J. C. Jeffrey, S. Houbrechts and A. Persoons, *Inorg. Chem.*, 1997, **36**, 3284–3292.

20 B. Mondal, M. G. Walawalkar and G. K. Lahiri, *J. Chem. Soc., Dalton Trans.*, 2000, 5209–4217.

21 (*a*) N. Gupta, N. Grover, G. A. Neyhart, W. Liang, P. Singh and H. H. Thorp, *Angew. Chem., Int. Ed. Engl.*, 1992, **31**, 1048–1050; (*b*) N. Grover, N. Gupta, P. Singh and H. H. Thorp, *Inorg. Chem.*, 1992, **31**, 2014–2020; (*c*) E. P. Kelson and P. Phengsy, *J. Chem. Soc., Dalton Trans.*, 2000, 4023–4024.

22 R. M. Berger and D. R. McMillin, *Inorg. Chem.*, 1988, **27**, 4245–4249.

23 A. P. B. Lever and E. S. Dodsworth, *Inorganic Electronic Structure Spectroscopy*, ed. E. I. Solomon and A. P. B. Lever, Wiley and Sons, New York, 1999, **vol. 2**, pp. 227–287.

24 M. Abe, Y. Sasaki, Y. Yamada, K. Tsukahara, S. Yano, T. Yamaguchi, M. Tominaga and T. Ito, *Inorg. Chem.*, 1996, **35**, 6724–6734.

25 V. J. Catalano, R. A. Heck, C. E. Immoos, A. Öhman and M. G. Hill, *Inorg. Chem.*, 1998, **37**, 2150–2157.

26 A. Dovletoglou, S. A. Adeyemi and T. J. Meyer, *Inorg. Chem.*, 1996, **35**, 4120–4127.

27 (*a*) C. K. Fair, in MolEN, An interactive intelligent system for crystal structure analysis, Nonius, Delft, The Netherlands, 1990; (*b*) C. K. Johnson, ORTEP-II: A FORTRAN Thermal Ellipsoid Plot Program for Crystal Structure Illustrations, Report ORNL-5138, Oak Ridge National Laboratory, Oak Ridge, TN, USA, 1976.

28 J. P. Collin, I. Dixon, J.-P. Sauvage, J. A. G. Williams, F. Barigelletti and L. Flamigni, *J. Am. Chem. Soc.*, 1999, **121**, 5009–5016.